Mössbauer, Crystallographic, and Density Functional Theoretical Investigation of the Electronic Structure of Bis-Ligated Low-Spin Iron(II) Phthalocyanines

Victor N. Nemykin,[a] Nagao Kobayashi,*[a] Victor Y. Chernii,[b] and Vitaly K. Belsky[c]

Keywords: Iron / Phthalocyanines / Mössbauer spectroscopy / Density functional calculations

We present the crystal structure of pcFe(4-methylpiperidine)$_2$ as a first example of a low-spin iron(II) phthalocyanine (pc) complex bis-axially coordinated by aliphatic amines. It is shown that electronic rather than steric effects are responsible for the elongation of the Fe–N(axial) bond in pcFeL$_2$ complexes. Using density functional theory, the electronic structures as well as Mössbauer isomer shifts and quadrupole splittings have been investigated for a large number of pcFeL$_2$ and pcFeL^{1}L^2 complexes, in which the axial ligands have varying electronic and steric properties. The electron charge densities and electric field gradients at the iron ion were evaluated using a locally dense basis approach with Wachters' all-electron basis set for the iron ion, the 6-311++G(2d) basis set for atoms directly bonded to the iron ion, the 6-31G(d) basis set for atoms two bonds away from the iron ion, and the 3-21G* basis set for all other atoms. A good correlation between the theoretical and experimental isomer shifts and quadrupole splittings has been observed for all the complexes tested. It has also been shown that the proposed model for the calculation of Mössbauer spectral parameters is adequate for the evaluation of the axial ligand conformation in cases of conformational flexibility in pcFeL$_2$ complexes.

Introduction

Iron-containing tetrapyrrole macrocycles and their analogues have been found to be capable of mimicking the active sites of a wide variety of biological enzymes.[1] Tetrabenzotetraazaporphyrin, i.e. phthalocyanine (pc), iron complexes have been the subject of widespread interest, both as homogeneous and heterogeneous catalytic systems with high oxygenating activity,[2] and have also been extensively studied as heme protein models[3] by virtue of their high thermal and chemical stability. The possibility of axial coordination and the stability of iron−axial ligand bonds are key features of these systems that play an important role in catalytic and model biological processes.[1−3] The nature of the central metal−axial ligand bonding in phthalocyanine iron complexes has been qualitatively discussed over the past 30 years. A large number of bis-axially coordinated low-spin iron(II) pcs (pcFeL$_2$ or pcFeL^{1}L^2) with aliphatic and heterocyclic nitrogen bases, isonitriles, phosphanes, and phosphites have been studied.[4−6] In principle, Mössbauer spectroscopy represents one of the most powerful methods for assessing the metal−axial ligand interaction in these systems. However, despite a large amount of experimental data concerning the Mössbauer spectra of iron pcs,[5,6] publications on the theoretical analysis of ^{57}Fe Mössbauer spectral parameters of these complexes are scarce, especially for bis-axially coordinated low-spin iron(II) pcs. This can be mainly attributed to two factors.[6] Firstly, only a few good X-ray crystallographic structures are available for pcFeL$_2$ or pcFeL^{1}L^2 complexes that can be used as initial structures for quantum mechanical calculations.[7] With a view to rectifying this situation, we present herein the first crystal structure of a low-spin iron(II) pc bis-axially coordinated by aliphatic amines. Secondly, the computation of energies, electronic structures, and properties of transition metal complexes requires consideration of electronic correlation effects.[8] However, for calculations of the electronic structures on systems of the size of pcFeL$_2$ or pcFeL^{1}L^2 (containing up to 97 atoms), all the usual electron correlation methods, based, for example, on multiconfigurational interaction, Möller−Plesset perturbation theory, or other algorithms, would require speeds typically as high as ca. N^5 (where N is the number of basis functions) and are still expensive. Fortunately, computational methods based on density functional theory (DFT) can be used as an alternative to conventional ab initio methods for large systems of this type because they include electron correlation effects in the exchange-correlation functional and are computationally very inexpensive. As has recently been shown, the simplest local density approximation (LDA) as well as the more precise B3LYP exchange-correlation functional generally give much better results for the ground-state properties of transition metal compounds, including porphyrins having structures that closely resemble those of pcs, than those obtained at the semiempirical or conventional ab initio Hartree−Fock levels.[9] In this paper, we present Mössbauer

[a] Department of Chemistry, Graduate School of Science, Tohoku University,
Sendai 980-8578, Japan
Fax: (internat.) + 81-22/217-7719
E-mail: nagaok@mail.cc.tohoku.ac.jp
[b] Vernadsky Institute of General and Inorganic Chemistry, Palladina Ave. 32/34, 252680 Kiev, Ukraine
[c] Karpov Institute of Physical Chemistry, Vorontsovo Pole 10, 103064 Moscow, Russia
Supporting information for this article is available on the WWW under http://www.wiley-vch.de/home/eurjic or from the author.

 © WILEY-VCH Verlag GmbH, 69451 Weinheim, 2001 1434−1948/01/0303−0733 $ 17.50+.50/0

spectra and the results of DFT calculations for a large number of bis-axially coordinated iron(II) pcs. In addition, X-ray crystallographic data are presented for a low-spin iron(II) pc coordinated by two aliphatic amines. In order to find the best computational method for the prediction of Mössbauer spectral parameters and to understand the origin of the differences in the spectroscopic data, comparative semiempirical, conventional ab initio, and DFT calculations have also been performed. In particular, we wanted to ascertain whether it is possible to reproduce a large difference in quadrupole splitting (ΔE_Q) among the complexes (from 0.56 to 2.28 mm s^{-1}), and to rationalize the influence of specific effects, such as the conformation of the axial ligands, on the Mössbauer spectral parameters. For these purposes, we chose the following pcs, in which the axial ligands have varying electronic and steric properties: pcFe(14en)$_2$ (**1**), pcFe(mepip)$_2$ (**2**), pcFe($BuNH_2$)$_2$ (**3**), pcFe(mim)$_2$ (**4**), pcFe(mepy)$_2$ (**5**), pcFe(*cyclo*-$C_6H_{11}NC$)$_2$ (**6**), pcFe(CO)(dmf) (**7**), and [pcFe$(CN)_2$]$^{2-}$ (**8**), where 14en, mepip, mim, and mepy are 1,4-diaminobutane, 4-methylpiperidine, *N*-methylimidazole, and 4-methylpyridine, respectively. As described below, the results represent the first successful theoretical analysis and prediction of Mössbauer spectral parameters in bis-axially coordinated low-spin iron(II) pcs.

Results and Discussion

Structural Aspects and Rotational Barriers

The SHELXTL-93 structure of pcFe(mepip)$_2$ (**2**) is shown in Figure 1. Atomic coordinates, as well as selected intramolecular distances and angles for this complex, are summarized in the Supporting Information (Tables 2 and 3) with the numbering scheme indicated in Figure 1. The structure of pcFe(mepip)$_2$ (**2**) is the first X-ray structure of an iron(II) pc to provide unprecedented stereochemical data on the coordination of aliphatic amines to iron pcs. In the recently reported X-ray structure of turnip cytochrome *f*, one of the axial ligands was found to be the α-NH_2 group of *Tyr*-1, and thus pcFe(mepip)$_2$ (**2**) may provide a useful starting point for delineating the role of aliphatic amino acids in biologically relevant amine complexes of iron porphyrins. In the unit cell of pcFe(mepip)$_2$ (**2**), four solvated mepip molecules are present in a chair conformation. The iron ion is coordinated by six nitrogen atoms that form an approximately square-bipyramidal structure. The essentially uniform Fe−N(pc) distance (1.93 Å) is consistent with a low-spin iron(II) configuration and is close to the corresponding distances found in other known bis(amino)-ligated iron(II) pcs such as pcFe(mim)$_2$ (**4**) and pcFe(mepy)$_2$ (**5**) (Table 1).[7a,7b] The Fe−N(mepip) distance (2.12 Å) is longer than that in any of the known iron(II) pcs bis-axially coordinated through the N, C, or O atoms of the ligands.[7] Two factors may be invoked to account for this bond elongation, namely steric interactions between protons of the axial ligand and the pc core, and electronic effects. Both of these are discussed below. The N(pc)−Fe−N(mepip) angles are close to 90° (the largest deviation is 1.85°). The phthalocyanine core is almost planar, keeping the interatomic distances close to those in pcFe(mim)$_2$ (**4**) and pcFe(mepy)$_2$ (**5**).[7] The axial ligands adopt a chair conformation with the intramolecular distances and angles close to those in solvated molecules present in the unit cell. The dihedral planes between the axial ligands are close to zero. This orientation of the axially coordinated mepip planes relative to the phthalocyanine core in the structure of **2** is fixed by the steric requirements imposed by the conformation of the solvated, as well as neighboring, axially coordinated mepip molecules. Any rotation of the axially coordinated ligands about the Fe−N(mepip) axis leads to a reduction in the non-bonding interactions between the carbon or hydrogen atoms of the axial ligands and the axially coordinated ligands of neighboring molecules of pcFe(mepip)$_2$ (**2**) and/or solvated mepip molecules. For example, rotation of the axial ligand about the *z* axis by 90° would result in unacceptably close non-bonding contacts (less that 2 Å) between the carbon atoms of the axial ligand and a nitrogen atom of a solvated mepip molecule. Such steric hindrance to the rotation of axial ligands in the crystal structure of pcFe(mepip)$_2$ (**2**) is well reproduced by rotational barrier calculations at the molecular mechanical and semiempirical levels. The results of calculations at the molecular mechanical level are summarized in Figure 2. Similarly qualitative results were obtained from semiempirical PM3 level calculations. Thus, the procedure described in the Experimental Section leads to estimated barriers for rotation of the axial ligands of 1.92 kcal mol^{-1}, 1.20 kcal mol^{-1}, and 2.54 kcal mol^{-1} at the MM+ level and of 2.07 kcal mol^{-1}, 1.71 kcal mol^{-1}, and 2.95 kcal mol^{-1} at the PM3 level for pcFe(mepip)$_2$ (**2**), pcFe(mim)$_2$ (**4**), and pcFe(mepy)$_2$ (**5**), respectively. Similar results have recently been reported for the barriers to rotation of axial ligands in predominantly planar or slightly distorted bis-axially coordinated iron(II) and iron(III) porphyrins.[9a,10] Thus, it is clear that in the gas phase, or in solution in the absence of any specific interactions between bis-axially coordinated iron(II) pcs and solvent molecules, the rotational barrier for rotations of axial ligands is invariably very small, in agreement with the room-temperature ^{1}H NMR spectral data.[4a−4e] On the other hand, for solvated mepip molecules the height of the rotational barrier of the axial ligand increases by more than two orders of magnitude according to both MM+ and PM3 calculations (Figure 2). Finally, it is important to delineate the factors that are responsible for the elongation of the Fe−N(axial) bond in pcFe(mepip)$_2$ (**2**) as compared with the corresponding distances in the complexes pcFe(mim)$_2$ (**4**) and pcFe(mepy)$_2$ (**5**). If steric interactions were to play a major role, as discussed previously[11] for tppFe(pip)$_2$, which contains an almost planar porphyrin core, the decrease in the Fe−N(axial) bond length would lead to a dramatic increase in the barrier to rotation of the axial ligand in pcFe(mepip)$_2$ (**2**). In order to reproduce this effect, model calculations on pcFe(mepip)$_2$ (**2**) were carried out in which the Fe−N(axial) bond length was shortened to 2.04 Å [as in pcFe(mepy)$_2$ (**5**)]. The results

showed that, in fact, the barrier to rotation of the axial ligand increases by less than 1.0 kcal mol^{-1} and that the total energies differ by less than 7 kcal mol^{-1}, both at the molecular mechanical and semiempirical levels. These results clearly indicate that the elongation of the Fe−N(axial) bond in pcFe(mepip)$_2$ (**2**) must stem from a difference in the electronic structure of the axial ligands in pcFe(mepip)$_2$ (**2**) compared to the situation in other pcFeL$_2$ and pcFeL^{1}L^2 complexes, in particular complexes pcFe(mim)$_2$ (**4**) and pcFe(mepy)$_2$ (**5**). Indeed, the Fe−N(axial) distances are roughly paralleled by the order of the magnitude of the sum of σ-donor and π-acceptor properties of the axial ligands: mepip > mepy > *cyclo*-$C_6H_{11}NC$ > CO.[5b,12]

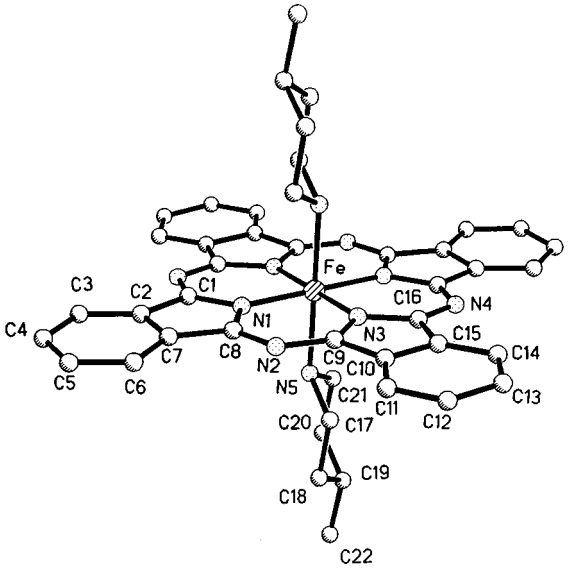

Figure 1. Perspective view of **2**; hydrogen atoms are omitted for clarity

Table 1. Structural data (distances in Å)

	1	**2**[a]	**3**	**4**[b]	**5**[c]	**6**[d]	**7**[e]	**8**[f]
Fe−N_{pc}	1.930	1.930	1.930	1.932	1.934	1.943	1.892	1.941
Fe−L_{ax}	2.080	2.119	2.080	2.012	2.040	1.911	1.72/2.07	1.960
$\|z_{max}\|$[g]	0.0	0.0	0.0	0.0	0.0	0.0	0.04	0.0

[a] This work. – [b] Ref.[7b] – [c] Ref.[7a] – [d] Ref.[7d] – [e] Ref.[7g] Fe−C(CO)/Fe−O(dmf). – [f] Ref.[7c] – [g] $|z_{max}|$ denotes the displacement of iron atom from the phthalocyanine N_4 plane.

Mössbauer Spectra of Bis-axially Coordinated Iron(II) Phthalocyanines

As for other low-spin ($S = 0$) iron(II) inorganic and organometallic compounds,[13] the Mössbauer spectra of bis-axially coordinated iron(II) phthalocyanines consist of one doublet,[5] the example shown in Figure 3 being typical. The quadrupole splitting, ΔE_Q, varies significantly from 0.56 mm s^{-1} in the complex [pcFe(CN)$_2$]$^{2-}$ (**8**) to 2.89 mm s^{-1} in pcFe(dabco)$_2$.[5d] The valence contribution (q_{val}) to ΔE_Q is approximately related to the anisotropy of the Fe(3d) and Fe(4p) shell occupations, as expressed by the Townes−Dailey approximation:[9a,13−16] $q_{val} =$

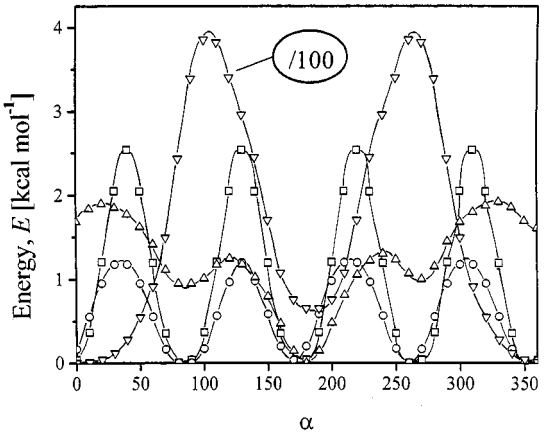

Figure 2. Barriers to axial ligand rotation in **2** (upward triangles), in **2** with solvated mepip molecules (inverted triangles), in **4** (circles), and **5** (squares), computed by a molecular mechanics (MM+) method

$^4/_7(1 - R)\langle r^{-3}\rangle_{3d}\{n(d_{xy}) + n(d_{x^2-y^2}) - n(d_{z^2}) - [n(d_{xz}) + n(d_{yz})]/2\} + {}^4/_5(1 - R)\langle r^{-3}\rangle_{4p}\{[n(p_x) + n(p_y)]/2 - n(p_z)\}$, where n(d) and n(p) are the effective populations of the respective iron orbitals, and $\langle r^{-3}\rangle$ is the expectation value of $1/r^3$ taken over the appropriate iron radial functions. For most bis-axially coordinated low-spin iron(II) macrocyclic complexes, such as pcs, porphyrins, and substituted dioximates, the valence contribution to ΔE_Q dominates[5,6a,9a] and hence the large (> 2.0 mm s^{-1}) quadrupole splitting seen in many pcFeL$_2$ complexes having a formal $(d_{xy})^2(d_{xz},d_{yz})^4$ electronic configuration is difficult to understand. Accordingly, in order to understand this phenomenon and to reproduce the large ΔE_Q values, comparative quantum chemical calculations were performed on the various pcFeL$_2$ and pcFeL^{1}L^2 complexes, as described in the next section.

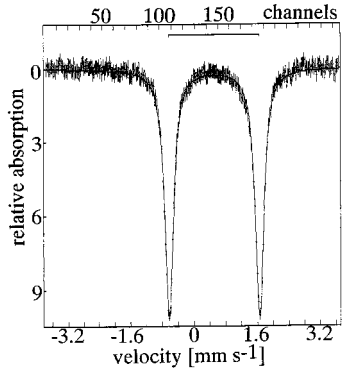

Figure 3. Room-temperature, zero-field Mössbauer spectrum of **2**

Density Functional Theory Calculations

Despite the large amount of experimental data on Mössbauer spectra of low-spin iron(II) pcs, only one theoretical study of quadrupole splittings on the basis of INDO semiempirical calculations has been published, although the parameters were not given.[6a] Moreover, to the best of our knowledge, there has been no report of a successful theoretical analysis of Mössbauer spectral parameters for low-spin

Table 2. Computed total charge electron densities for the ^{57}Fe atoms in complexes **1−8**, together with the calculated and experimental Mössbauer quadrupole splittings (in mm s^{-1}) and asymmetry parameters

		1a	1b	2	3	4	5	6	7	8a	8b
δ	Expt.	0.48[a]		0.53[a]	0.51[a]	0.52[a]	0.52[b]	0.39[c]	0.35[d]	0.38[e]	
ΔE_Q	Expt.	1.84		+2.28[f]	1.97	1.71	+1.96[g]	+0.69[h]	+1.56[i]	0.56	
η	Expt.	0.0		0.0	0.0	0.0	0.0	0.0	0.0	0.0	
ΔE_Q	*Z*/*S*[j]	1.02		0.97	1.09	0.88	0.96	0.40	1.51	0.28	
ΔE_Q	RHF			1.33		0.76					
ΔE_Q	B3LYP	1.92	1.99	2.18	2.02	1.72	1.94	0.55	1.84	−0.02	0.51
η	B3LYP	0.0	0.0	0.0	0.0	0.0	0.0	0.1	0.0	0.0	0.4
ρ(o)	B3LYP G98	11616	11616	11616	11616	11616	11616	11617	11617	11617	11617
ρ(o)	B3LYP GS	11615.94	11615.99	11615.84	11616.03	11615.91	11615.94	11616.51	11616.77	11616.65	11616.66
ΔE_Q	LSDA	2.304		2.69	2.20	2.10	2.24	0.87	1.93	0.26	0.78
η	LSDA	0.1		0.0	0.0	0.0	0.0	0.1	0.0	0.0	0.2
ρ(o)	LSDA G98	11566		11566	11566	11566	11566	11567	11567	11567	11567
ΔE_Q	LDA	1.90		2.46	2.53	2.17	2.30	0.91	2.10	0.28	0.95
η	LDA	0.0		0.0	0.0	0.0	0.1	0.1	0.0	0.0	0.3
ρ(o)	LDA G98	11579		11579	11579	11579	11579	11580	11580	11580	11580

[a] This work. − [b] Ref.[5a] − [c] Ref.[5d] − [d] Ref.[5e] − [e] Ref.[5f] − [f] Based on sign determined for $pcFe(pip)_2$, ref.[5i] − [g] Based on sign determined for $pcFe(py)_2$, ref.[4c] − [h] Based on sign determined for $pcFe(mesNC)_2$, ref.[5d] − [i] Based on sign determined for pcFe(CO)(MeOH), ref.[5i] − [j] Abbreviations: *Z*/*S* is Zerner's INDO-S parameterization; RHF is the ab initio Hartree−Fock level with Wachters' all-electron basis set on iron and the 6−311+G(2d) basis set on all other atoms; G98 is Gaussian-98W; GS is GAMESS (USA).

iron(II) pcs. In view of this, the Mössbauer spectral parameters for the complexes $pcFe(mepip)_2$ (**2**) and $pcFe(mim)_2$ (**4**), for which relatively large quadrupole splittings were observed compared to other low-spin iron(II) pcs, have been analyzed theoretically, and the results have been compared by quantum chemical calculations at the following levels of theory: (i) semiempirical ZINDO/S,[17] (ii) conventional ab initio [with the same basis set as discussed for DFT methods, as well as with Wachters' all-electron basis set for iron and 6-311+G(2d) for all other atoms], (iii) DFT methods with B3LYP, LDA, and LSDA EC functionals. As can be seen from the results presented in Table 2, the electric field gradients obtained from both semiempirical and conventional ab initio methods show a marked deviation from the experimental values, while those obtained from the DFT methods are much closer. As a consequence, in the following we will discuss and compare only the results of the DFT calculations.

Orbital Energies

The order of the orbital energies is shown in Table 3, in the Supporting Information (Tables 4 and 5), and Figure 4 and Figure 5. In general, the order of metal-centered orbitals reflects the splitting pattern of distorted octahedral coordination of the central ion. The "t_{2g}" manifold of the Fe(3d) orbitals is split into an almost degenerate d_{xz} and d_{yz} pair and a d_{xy} orbital, except in the case of $[pcFe(CN)_2]^{2-}$ (**8**), while the "e_g" manifold is split into d_{z^2} and $d_{x^2-y^2}$ orbitals. Furthermore, in all cases the LUMO "e_g" orbitals are pc-centered as in other metal-containing pcs.[21] However, the relative energies of the metal-centered orbitals as well as the pc-centered orbitals were found to be strongly dependent on the EC functional used. Thus, when the B3LYP EC hybrid functional was used (Figure 4), the pc "a_{1u}" (in D_{4h} notation) orbital was found to be the HOMO for all the complexes, except in the case of

Table 3. Calculated orbital energies (eV) for complexes **1−8** using the B3LYP hybrid EC functional

Orbital	1	2	3	4	5	6	7	8
$d_{x^2-y^2}$	1.133	1.250	1.209	1.447	1.184	1.004	0.719	6.600
d_{z^2}	0.365	0.091	−0.065	0.749	0.306	0.478	−0.422	6.598
pc "b_{1u} (π*)"	−0.440	−0.677	−0.676	−0.399	−0.602	−0.602	−0.657	4.224
pc "e_g (π*)"	−1.966	−2.219	−2.230	−1.904	−2.120	−2.128	−2.281	3.056
	−1.974	−2.231	−2.239	−1.904	−2.122	−2.130	−2.278	3.056
pc "a_{1u} (π)"	−4.406	−4.628	−4.663	−4.364	−4.523	−4.591	−4.688	0.548
d_{xz}	−4.853	−5.058	−5.151	−4.841	−5.156	−5.306	−5.898	0.591
d_{yz}	−4.888	−5.120	−5.168	−4.843	−5.167	−5.310	−5.902	0.591
d_{xy}	−5.269	−5.367	−5.415	−5.090	−5.437	−5.498	−6.037	0.037
pc "a_{2u}(π)"	−5.893	−6.252	−6.316	−5.991	−6.193	−5.885	−6.522	0.015
2p(Fe)	702.80	702.73	702.79	702.50	702.97	703.19	703.89	697.49
3s(Fe)	92.14	92.16	92.21	91.89	92.28	92.49	93.26	86.77
Δ_{cf}	5.237	5.180	5.095	5.591	5.468	5.786	5.478	6.007
Δ_{ct}	4.431	4.412	4.484	4.443	4.560	4.706	5.243	3.633
Δ_{Qband}	2.436	2.378	2.428	2.460	2.402	2.462	2.408	2.508
Δ_{Bband}	3.923	4.027	4.071	4.087	4.072	3.756	4.242	3.041
$\Delta_{a1u-a2u}$	1.487	1.624	1.653	1.627	1.670	1.294	1.834	0.533

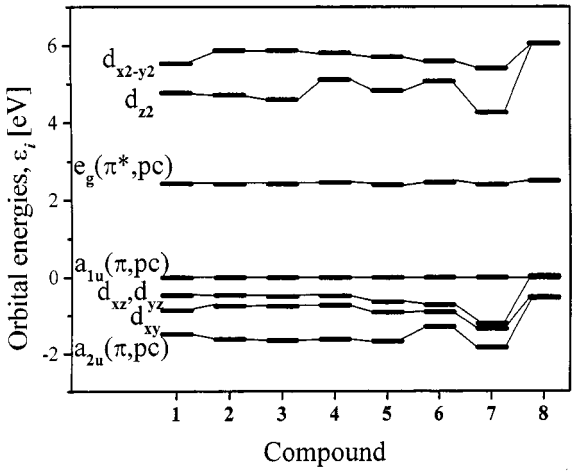

Figure 4. The ground-state MOs of complexes **1**−**8** [relative to "a_{1u}" (pc) orbital] with predominant Fe(3d) character, as well as the most important pc-centered MOs, as obtained by B3LYP DFT calculations

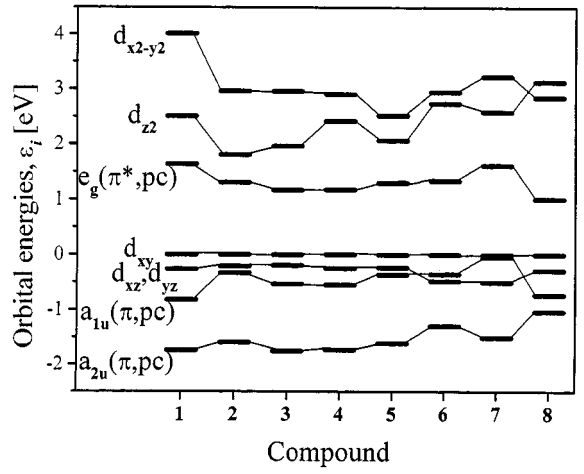

Figure 5. The ground-state MOs of complexes **1**−**8** (relative to d_{xy} orbital) with predominant Fe(3d) character, as well as the most important pc-centered MOs, as obtained by LSDA DFT calculations

$[pcFe(CN)_2]^{2-}$ (**8**) where the d_π orbitals are slightly higher in energy and are thus the HOMOs. For **1**−**8**, the d_{xz} and d_{yz} orbitals are higher in energy compared to d_{xy}, while the $d_{x^2-y^2}$ orbital is always higher in energy than d_{z^2}. When LDA and LSDA EC functionals were employed (Figure 5), the order of the orbital energies was found to be roughly similar, but differed in a few respects. Thus, the near-degenerate "d_π" orbitals are always lower in energy than the d_{xy} orbital, which is the HOMO. The $d_{x^2-y^2}$ orbital is higher in energy than the d_{z^2} orbital for **1**−**7**, while in the case of $[pcFe(CN)_2]^{2-}$ (**8**) the order of these orbitals is reversed. As can be seen in Figure 4 and 5, the splitting between the $d_{x^2-y^2}$ and d_{z^2} orbitals is considerably smaller for the complexes pcFe(*cyclo*-$C_6H_{11}NC)_2$ (**6**) and $[pcFe(CN)_2]^{2-}$ (**8**). The main reason for this is the destabilization of the iron d_{z^2} orbital due to the shorter iron−axial ligand distances as compared to those in the other tested complexes. In the case of $[pcFe(CN)_2]^{2-}$ (**8**), strong electron donation from the negatively charged cyano groups also serves to destabilize the d_{z^2} orbital. In the case of complexes pcFe(*cyclo*-$C_6H_{11}NC)_2$ (**6**) and pcFe(CO)(dmf) (**7**), which contain at least one axial ligand with strong π-back-donating properties, the d_{xz} and d_{yz} orbitals are significantly stabilized and have lower energies than the pc-centered "a_{1u}" orbital.

It is interesting to compare the calculated iron 2p and 3s orbital energies with the experimentally determined ionization potentials (IPs) (XPS experiments) for the $pcFe(im)_2$ ($Fe_{2p3/2}$: 708.0 eV; Fe_{3s}: 92.5 eV) and $pcFe(3mepy)_2$ ($Fe_{2p3/2}$: 708.1 eV; Fe_{3s}: 92.3 eV) complexes.[19] The reverse-signed 2p and 3s iron orbital energies computed for complexes **1**−**8** [Table 3 and Supporting Information (Tables 4 and 5)] parallel the IP values obtained from the XPS data. In particular, the closest values were obtained using the B3LYP EC functional.

The crystal field splittings, Δ_{cf}, defined as the differences between the orbital energies of d_π (average value) and d_{z^2} for the B3LYP EC functional (Figure 4) or d_{xy} and d_{z^2} {$d_{x^2-y^2}$ for $[pcFe(CN)_2]^{2-}$ (**8**)} for the LDA and LSDA EC functionals (Figure 5) are larger than 1.8 eV, in agreement with the observed low-spin ground state for **1**−**8** (in general, the value of Δ_{cf} parallels the values in the spectrochemical series).[20] It is well known that in the electronic spectra of $pcFeL_2$ and $pcFeL^1L^2$ complexes, the band at around 2.95 eV can be assigned as a metal-to-ligand charge transfer (MLCT) band [d_{xz}, d_{yz} → "b_{1u}" (π*, pc)] since it is sensitive to the nature of the axial ligand.[4f,21] Using the LDA and LSDA EC functionals, the estimated energies of the MLCT bands were in qualitative agreement with the available experimental data, while with the B3LYP EC functional, the obtained values reflected a strong overestimation of the MLCT band energies, which is typical of ground-state calculations with hybrid DFT EC functionals.[22] For all the tested EC functionals, the pc "a_{1u}" orbital was found to be higher in energy than the pc "a_{2u}" orbital and the orbital separation was of the order of 1 eV or more {except for complex $[pcFe(CN)_2]^{2-}$ (**8**)}, consistent with the fact that the lowest energy π-π* transition has an essentially pure "a_{1u}" (π, pc) → "e_g"(π*, pc) configuration.[21]

Isomer Shifts and Electric Field Gradients

The following five quantities can be derived from Mössbauer experiments, as well as theoretical calculations using SCF wavefunctions:[13] isomer shift (δ), quadrupole splitting (ΔE_Q), the sign of the principal component, V_{zz}, of the EFG tensor, the direction of V_{zz}, and the asymmetry parameter (η). The isomer shift in Mössbauer spectroscopy depends on the electron charge density, ρ(0), at the nucleus and is proportional to changes in ρ(0) with respect to reference compounds. Thus, $\delta = \alpha[\rho(0) - \rho_r(0)]$, where α is a calibration constant and ρ(0) and $\rho_r(0)$ are the electron charge densities at the nuclei in the sample and reference compounds, respectively.[13] For quantum chemical calculations, the $\rho_r(0)$ value is usually replaced by a constant, β, and thus δ is calculated as $\delta = \alpha[\rho(0) - \beta]$. In the ideal case, β corresponds to the electron charge density at the Mössbauer nucleus in the reference compound.[13,23] A good correlation was found when plotting the isomer shift

values against the calculated total electron charge densities on the iron atoms for complexes **1−8** (Figure 6). The calibration constant, α, was evaluated as −0.192 a_o^3 mm s^{-1} for the eight points, with a correlation coefficient r^2 of 0.980 and an r.m.s. error of 0.016 mm s^{-1}. This obtained value of α is close to that recently published and used for CASSCF ab initio calculations of Mössbauer spectral parameters for iron porphyrins (−0.166 a_o^3 mm s^{-1})[23a] and other iron-containing inorganic and organometallic compounds.[24] Moreover, the value obtained for constant β (Figure 6) is close to the calculated total electron charge density at the iron atom in sodium nitroprusside (11617.77 a_o^{-3}). When the calculated value for sodium nitroprusside ρ(0) was included in the ρ(0)/δ correlation analysis, the correlation coefficient did not change ($r^2 = 0.981$), but α changed significantly from −0.19 to −0.26 a_o^3 mm s^{-1}. The latter value of α is closer to that found by Trautwein et al. for some iron-containing inorganic compounds (−0.31 to −0.38 a_o^3 mm s^{-1}).[25] The calibration constant α can also be written as $\alpha = (4Ze^2R^2c/5E_\gamma)\cdot(\delta R/R) = C\cdot(\delta R/R)$,[13] where R is the average nuclear radius and δR is the change in radius on going from the ground to the excited state. Having estimated α from a ρ(0)/δ correlation analysis and calculated the total electron charge density for sodium nitroprusside, which is used as a reference compound, it is possible to estimate the value of $\delta R/R$ in order to support our isomer shift calculations on $pcFeL_2$ and $pcFeL^1L^2$ complexes. Using the value of $C = 0.3083\cdot10^3$ a_o^3 mm s^{-1} obtained by Alton and Swift,[24c] the $\delta R/R$ values were estimated (average for **1−8**) as $-6.16\cdot10^{-4}$ and $-8.43\cdot10^{-4}$ when α is −0.19 and −0.26 a_o^3 mm s^{-1}, respectively. Both these values are in reasonable agreement with previously published results.[24] Although the computed values of α and $\delta R/R$ estimated from the correlation analysis are different, the present results are very promising because they suggest that Mössbauer isomer shifts in iron pcs, and probably in other iron-containing compounds as well, can be calculated with high accuracy using modern DFT methods.

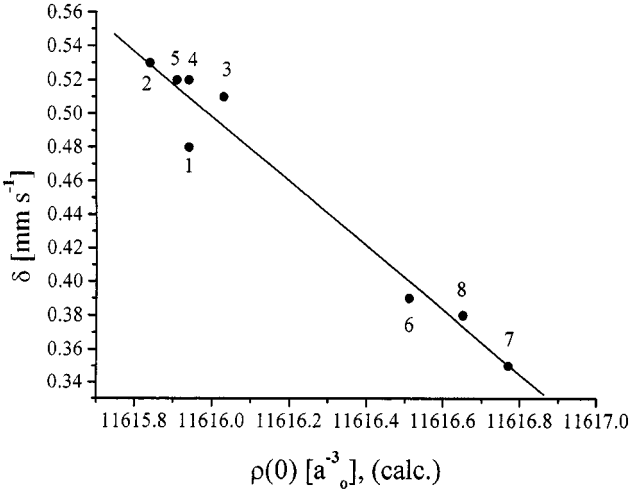

Figure 6. Correlation between the observed Mössbauer isomer shifts and the calculated total electron densities at the ^{57}Fe nucleus by the B3LYP DFT method; numerical values are given in Table 2

The Mössbauer quadrupole splittings and asymmetry parameters, η, for compounds **1−8**, calculated using the locally dense basis set approach in conjunction with the B3LYP, LSDA, and LDA EC functionals are presented in Table 2, while those calculated with the B3LYP EC functional are shown graphically in Figure 7. The results of our DFT calculations using the B3LYP EC functional demonstrate that the magnitude of the ΔE_Q values, the sign and orientation of the principal component of the EFG tensor, and the η values, are all in agreement with the experimental data. A correlation coefficient of $r^2 = 0.982$, with an r.m.s. error of 0.14 mm s^{-1}, has been found between the predicted and experimental ΔE_Q values for complexes **1−8**. These results are very promising, since they suggest that DFT methods can now be applied with some reliability to predicting both Mössbauer quadrupole splittings and Mössbauer isomer shifts in large systems such as phthalocyanines, for which other methods based on semiempirical and conventional ab initio quantum mechanical levels have hitherto proved inadequate. For example, for the complex $pcFe(mepip)_2$ (**2**), we have computed ΔE_Q and δ values of 2.18 and 0.52 mm s^{-1}, respectively, which can be quite favorably compared with the experimental values of 2.28 and 0.53 mm s^{-1}. Similarly, for complex $pcFe(cyclo\text{-}C_6H_{11}NC)_2$ (**6**), even though the EFG is much smaller, there is likewise good accord between the computed (0.55 and 0.35 mm s^{-1}) and experimental (0.69 and 0.39 mm s^{-1})[5d] values. Among complexes **1−8**, the computed and experimental ΔE_Q values only differ significantly in the case of the complex $[pcFe(CN)_2]^{2-}$ (**8**) (marked as **8a** in Table 2 and indicated by an unfilled circle in Figure 7); this large deviation could originate from the uncompensated lattice effects of two positively charged counterions, as well as from deficiencies in the basis sets and the functional used. Indeed, when, for example, two sodium ions were placed in the positions of the cationic nitrogen atoms of PNP counterions, as determined experimentally for $(PNP)_2[pcFe(CN)_2]$,[7c] the calculated ΔE_Q value was found to be in excellent agreement with the experimental data (marked as case **8b** in Table 2). The large η value calculated in the case of **8b** can easily be explained by taking into consideration the fact that in the actual crystal of $(PNP)_2[pcFe(CN)_2]$, the iron pc is symmetrically surrounded by four PNP cations,[7c] whereas in our model calculation only two sodium ions were used in order to compensate for the negative charge of the $[pcFe(CN)_2]^{2-}$ moiety. The observation that V_{zz} is directed along the Na−Na axis supports this explanation. As pointed out in the literature,[4a][5a][5b] the axial ligand in the complex $pcFe(14en)_2$ (**1**) is probably stabilized through intramolecular hydrogen bond formation. It is thus interesting to compare the experimental Mössbauer spectral parameters with those calculated for the open-chain (**1a**) and intramolecularly hydrogen-bonded conformations (**1b**). The calculated Mössbauer spectral parameters for **1a** are close to those calculated for the complex $pcFe(BuNH_2)_2$ (**3**), for which only an open-chain conformation is possible. On the other hand, the calculated Mössbauer spectral parameters for **1b** are in close agreement with the experimental data, sup-

porting the previously proposed hypothesis concerning the possibility of intramolecular hydrogen bonding in this complex. Additional evidence concerning the axial ligand conformation in pcFe(14en)$_2$ (**1**) can be obtained from a comparison of the experimental ^{1}H NMR spectra of pcFe(14en)$_2$ (**1**) and pcFe(BuNH$_2$)$_2$ (**3**) and the computed isotropic shifts for the protons of the axial ligands. It is well known that in the ^{1}H NMR spectra of pcFeL$_2$ complexes the protons of the axial ligands are strongly shielded by the ring current of the pc ring, this effect depending on the electronic structures of the axial ligands and their positions in relation to the pc plane.[4a−4e] The experimental chemical shifts for the coordinated NH$_2$ protons in pcFe(14en)$_2$ (**1**) and pcFe(BuNH$_2$)$_2$ (**3**), as well as the calculated chemical shifts and shieldings are summarized in Table 4, together with the calculated NMR parameters for ^{57}Fe. Again, the calculated chemical shifts for **1a** and pcFe(BuNH$_2$)$_2$ (**3**) are close, while the values for **1b** differ significantly in accord with the experimental data. Finally, the computed ^{57}Fe chemical shifts have reasonable values, as judged on the basis of the available experimental and calculated data for bis-axially coordinated iron(II) porphyrins.[9c,26] Since the calculated η values for complexes **1**−**8** are small, and the direction of V_{zz} corresponds almost exactly with the molecular z axis, in agreement with the experimental data,[4c,4d] the V_{zz} components of the EFG can be divided into the so-called valence, covalence, and lattice contributions.[9a,14,15] The valence contribution is approximately proportional to the anisotropy of the Fe(3d) and Fe(4p) shell occupations. The covalence contribution is almost proportional to the Fe−ligand overlap population, while the ligand contribution arising from the cores and valence electrons of all ligand atoms is roughly proportional to the charge on the atom of the ligand directly coordinated to the iron and the Fe−ligand distance as Z/r^3. Taking all these factors into consideration, it appears possible to discuss the influence of each contribution on the EFG in complexes **1**−**8**. Unfortunately, however, as discussed in the literature,[27,28] the Mulliken population and charge distribution analysis are completely inappropriate for systems containing a large number of diffuse Gaussian-like functions. Thus, considering the fact that for bis-axially coordinated iron pcs and porphyrins, particularly for those with experimentally large ΔE_Q values, the valence contribution usually dominates over the covalent and ligand contributions,[9a] the anisotropy of the Fe(3d) and Fe(4p) shell occupations can be expected to be around 0.3−0.5 electrons for complexes **1**−**5** and **7**. However, a Mulliken population analysis gave an anisotropy of Fe(3d) shell occupation of no more than 0.23 electrons. The covalent contribution, which is based on the Mulliken population analysis, is also inappropriate because the overlap populations have negative (!) values for all the Fe−ligand bonds in all the cases tested and, of course, do not have any physical meaning. The most attractive alternative to the Mulliken population analysis is based on the use of Natural Bond Orbital (NBO) population and charge distribution analysis.[28] However, the NBO package, as implemented in the Gaussian-98 program family and GAMESS (USA) software, is unable to operate with such large and highly covalent systems as found in phthalocyanines. Since the Gaussian-98W program is based on Gaussian-type basis functions, the next questions to be addressed are the influence of various basis sets, particularly on the iron atom, and of the functionals on the calculated EFG components and thus the ΔE_Q values. From our comparative calculations of the EFG components for the complexes pcFe(mepip)$_2$ (**2**) and [pcFe(CN)$_2$]$^{2-}$ (**8**) using the Wachters−Hay all-electron basis set (611111111/51111/311) for the iron ion, with and without the inclusion of diffuse functions, and using the original Wachters' all-electron basis set for the iron ion,[16,17] with and without the inclusion of polarization functions, it can be concluded that the influence of diffuse and polarization functions is small, and that the ΔE_Q values computed with the Wachters−Hay all-electron basis set are in better agreement with the experimental data [Supporting Information (Table 6)]. The ΔE_Q values calculated with pure DFT functionals (LDA and LSDA), as well as those estimated from Gaussian-98W calculations of ρ(0), are presented in Table 2. Inspection of these results reveals that the estimated values of ρ(0) are in good agreement with the expected values, while both functionals are systematically overestimated with respect to the experimentally observed ΔE_Q values for complexes **1**−**7**. However, in both cases, a good correlation between calculated and experimental ΔE_Q values is observed, with correlation coefficients r^2 of 0.957 and 0.993 and r.m.s. errors of 0.18 and 0.09 mm s^{-1} for the LDA and LSDA EC functionals, respectively. One of the advantages of the hybrid DFT B3LYP EC functional is that it is not necessary to take Sternheimer corrections into consideration when ΔE_Q values are computed from the EFG tensor components. On the other hand, for pure DFT methods, Sternheimer corrections must be applied when ΔE_Q values are computed, at least for the LDA functional, as pointed out by the authors.[9a,14,15] Since it is impossible to separate valence, covalence, and lattice contributions to the EFG using the Gaussian-98W

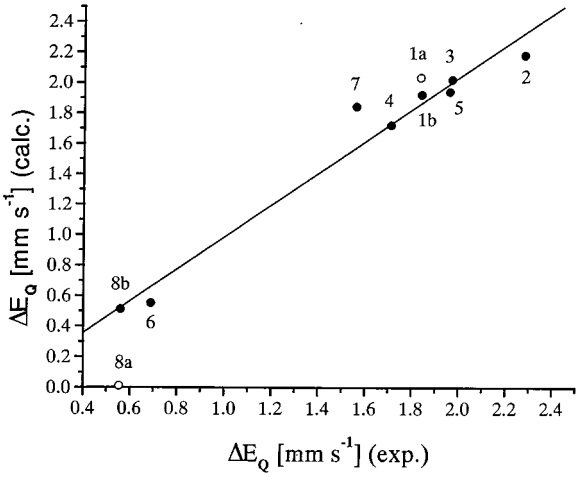

Figure 7. Correlation between the experimental and calculated (by the B3LYP DFT method) Mössbauer quadrupole splittings in complexes **1**−**8**; numerical values are given in Table 2

Table 4. Calculated and experimental ^{1}H (coordinated NH_2 group) and ^{57}Fe NMR shielding (ppm) for complexes **1** and **3**

Complex	Atom	Shielding tensor element. σ_{11}	σ_{22}	σ_{33}	Isotropic shielding σ_i	Isotropic shift δ_i Calcd.	Exp.
1a	Fe[a]	−14435	−14228	−7326	−11996	9084	
	NH_2 [b]	35.4265	38.2657	47.2148	40.3023	−8.38	−6.58
1b	Fe	−13944	−13810	−6634	−11462	8551	
	NH_2	29.9200	37.0061	47.1299	38.0187	−6.10	−6.58
3	Fe	−14635	−14538	−7305	−12159	9247	
	NH_2	36.8145	39.6581	47.2216	41.2314	−9.31	−7.44

[a] The isotropic shifts are obtained from the computed absolute shielding as: $\delta = -2912 - \sigma$, where the value of $\delta = -2912$ refers to the computed absolute shielding in $Fe(CO)_5$. − [b] The isotropic shifts are obtained from the computed absolute shielding as: $\delta = 31.9197 - \sigma$, where the value of $\delta = 31.9197$ refers to the computed absolute shielding of the protons in TMS at the B3LYP/6−31G(d) level.

and GAMESS (USA) programs, we were unable to accurately calculate ΔE_Q values for complexes **1**−**8** applying Sternheimer corrections, even at the limits of the simple Townes−Dailey approximation.[16,29]

Thus, it is concluded that DFT methods, particularly employing the B3LYP EC functional, are now able to reproduce and predict the Mössbauer spectral parameters of bis-axially coordinated iron(II) pcs with high accuracy, in contrast to semiempirical and conventional ab initio methods. The hybrid B3LYP EC functional can be recommended as the best approximation for the evaluation of total electron charge density and electric field gradient on a Mössbauer nucleus using the Gaussian-98W program, while the LDA and LSDA EC functionals are only useful with software implementing an alternative to Mulliken population analysis algorithms.[9a,14,15]

Conclusions

In this paper, we have discussed the relationship between the nature of the axial ligands in bis-axially coordinated iron(II) phthalocyanines and their electronic structures, structural, and Mössbauer spectral parameters. The first example of a crystal structure of a low-spin iron(II) pc bis-axially coordinated by aliphatic amines has been presented, and the reasons for the observed elongation of the Fe−N(ax) bond length have been discussed. The electronic structures of numerous $pcFeL_2$ and $pcFeL^1L^2$ complexes have been assessed on the basis of density functional theory calculations. The results constitute the first accurate calculations of Mössbauer quadrupole splittings and isomer shifts for bis-axially coordinated low-spin iron(II) phthalocyanine complexes by means of density functional theory methods. A good correlation between the experimental and theoretical values has been obtained using the hybrid B3LYP EC functional, while with the pure DFT LDA and LSDA functionals, it has been found that Sternheimer corrections need to be taken into consideration when quadrupole splittings are computed. Of particular interest is the reproduction of the Mössbauer spectral parameters of complexes with conformationally flexible axial ligands.

Experimental Section

Synthesis: Compounds **1**−**4** were synthesized according to standard methods.[4a−4c][5a−5c] All the complexes were characterized by their UV/Vis, ^{1}H NMR, and Mössbauer spectra, as well as by elemental analysis [Supporting Information (Table 1)]. In addition, an experimental geometry for $pcFe(mepip)_2$ (**2**) was determined by an X-ray crystallographic analysis.

X-ray Crystallography: A single crystal of $pcFe(mepip)_2$ (**2**) was obtained by slowly evaporating the solvents from a benzene/heptane (1:3, v/v) solution of the complex over a period of a week. Diffraction data were collected with a CAD-4 diffractometer using Mo-K_α radiation ($\lambda = 0.71073$ Å). The structure was solved by full-matrix least-squares techniques on F^2 for all data, with anisotropic thermal parameters for non-hydrogen atoms and isotropic parameters for hydrogen atoms. All calculations were performed using the SHELXTL-93 software.[30] General information concerning the crystal structural determination is given in Table 5. Crystallographic data (excluding structural factors) for **2** have been deposited at the Cambridge Crystallographic Data Centre (CCDC) as supplementary publication no. CCDC-145879. Copies of the data

Table 5. Crystal data and structure refinement for **2**

Empirical formula	$C_{56}H_{68}FeN_{12}$
Formula mass	965.08
T	293 K
Crystal system	monoclinic
Space group	$P2(1)/a$
Unit cell dimensions	$a = 11.792(2)$ Å
	$b = 17.213(3)$ Å
	$c = 12.645(3)$ Å
	$\beta = 102.58(3)°$
Volume	2505.0(9) Å^3
Z	4
Standards number	3
Standards interval time	60 min
Standards decay	0.01%
Density (calculated)	1.279 mg/m^3
Absorption coefficient	0.352 mm^{-1}
$F(000)$	1028
Crystal size	0.42 × 0.31 × 0.28 mm
θ range for data collection	1.65−22.47°
Index ranges	$-12 \le h \le 12$
	$0 \le k \le 18$
	$0 \le l \le 13$
Reflections collected	2036
Independent reflections	1925 [R(int.) = 0.0124]
Data/restraints/parameters	1925/0/434
Final R indices [$I > 2\sigma(I)$]	$R_1 = 0.0305$ $wR_2 = 0.0843$
R indices (all data)	$R_1 = 0.0305$ $wR_2 = 0.0843$
Extinction coefficient	0.0000(4)
Largest diff. peak and hole	0.244 and −0.232 eÅ^{-3}

can be obtained free of charge on application to the CCDC, 12 Union Road, Cambridge CB2 1EZ, U.K. [Fax: (internat.) + 44-1223/336-033; E-mail: deposit@ccdc.cam.ac.uk].

Mössbauer Spectroscopy: Mössbauer spectra were recorded using a GRS-4M spectrometer in constant acceleration mode. The source was ^{57}Co in a chromium matrix with an initial activity of 50 mCi. Isomer shifts were referenced to sodium nitroprusside at 298 K (the conversion factor from sodium nitroprusside to iron foil is -0.257 mm s^{-1}).

Computational Aspects: Total electron charge density and electric field gradient calculations were carried out using Gaussian-98W software.[31] In order to negate convergence problems, the following procedures were used for the energy convergence and electric field gradient calculations: Step 1: All atoms were represented by a 3-21G* basis set at the Hartree−Fock level. Step 2: As Step 1, but iron was represented by a Wachters−Hay all-electron basis set (611111111/51111/311) using the scaling factors of Raghavachari and Trucks,[32] and the 6-31G* basis set was used for all atoms directly attached to or two bonds away from iron. Step 3: As Step 2, but using the respective exchange-correlation functional. The following exchange-correlation (EC) functionals were used for the DFT calculations: Becke's three-parameter exchange functional with the Lee, Parr, and Yang correlation functional (B3LYP),[33] the Local Density Approximation (LDA) functional,[34] and the Local Spin Density exchange functional with the Vosko, Wilk, and Nusair correlation functional (LSDA).[35] Step 4: As Step 3, but a 6-311++G(2d) basis set was used for all atoms directly attached to iron. Since Raghavachari and Trucks recommended both scaling and the inclusion of diffuse functions when using a Wachters−Hay basis set for the first transition row elements,[32] we compared electric field gradient calculations on the complexes pcFe(mepip)$_2$ (**2**) and [pcFe(CN)$_2$]$^{2-}$ (**8**) using a Wachters−Hay basis set for iron with and without diffuse functions. Moreover, since the Wachters−Hay basis set implemented in the Gaussian-98W program and the set originally reported by Wachters[36] are different, we also compared electric field gradient calculations on the complexes pcFe(mepip)$_2$ (**2**) and [pcFe(CN)$_2$]$^{2-}$ (**8**) using the original Wachters' all-electron basis set for iron (62111111/331211/3111), with and without the inclusion of polarization functions.[37] A more detailed discussion concerning the influence of different Wachters' basis sets at the iron atom on the electric field gradient tensor elements in the complexes pcFe(mepip)$_2$ (**2**) and [pcFe(CN)$_2$]$^{2-}$ (**8**) is given in the Results and Discussion section. The total electron charge densities on the iron atoms were estimated using Gaussian-98W software with the help of the atoms-in-molecules (AIM) algorithm.[21] Since the current codes of AIM included in the Gaussian-98W program can only operate up to five digits when total electron densities are computed (this leads to an error of 0.1−0.2 mm s^{-1} in the isomer shift calculations), the total electron charge densities on the iron atoms were calculated more precisely using GAMESS (USA) software[38] with the help of converged wavefunctions obtained from the previous DFT calculations [DFT is not currently included in GAMESS (USA)]. The components of the electric field gradient tensor (EFG), V_{ii}, were directly calculated using a Gaussian-98W program based on the following expression: $V_{ij} = \partial^2/\partial_{xi}\partial_{xj}[\Sigma Z_A e/(|r_A - r_{Fe}|) - \int e\rho(r)/(|r - r_{Fe}|)dr]$, where r_{Fe} is the position vector of the iron nucleus, ρ(r) is the first-order density matrix of electrons, and r_A and Z_A are the position vector of the nucleus of atom A and the nuclear charge, respectively. The measured ΔE_Q is related to the major component, V_{zz}, of the EFG tensor according to the following expression[33] where e is the electron charge, Q is the quadrupole moment of the $I^* = 3/2$ 14.4 keV excited state, and η is the asymmetry parameter [$\eta = |V_{xx} - V_{yy}|/|V_{zz}|$ ($V_{zz} > V_{yy} > V_{xx}$)].

$$\Delta E_Q = (1/2)eQV_{zz}(1 + \eta^2/3)^{1/2}$$

The magnitude of the nuclear quadrupole moment Q was chosen as 0.16 barn on the basis of the most recently determined value.[9b,39] This value is also close to that used by Trautwein's group (0.15 barn) for calculations of Mössbauer spectral parameters using an LDA EC functional.[9a,14,15] As recently shown[9b−9d] for DFT calculations with a B3LYP hybrid EC functional, Sternheimer corrections do not have to be taken into account when ΔE_Q is predicted on the basis of the DFT calculations. Experimentally determined geometries for pcFe(mepip)$_2$ (**2**), pcFe(mim)$_2$ (**4**), pcFe(mepy)$_2$ (**5**), pcFe(*cyclo*-C$_6$H$_{11}$NC)$_2$ (**6**), pcFe(CO)(dmf) (**7**), and [pcFe(CN)$_2$]$^{2-}$ (**8**) were used,[7] with the modification that C−H and N−H bond lengths were extended to typical values (1.05−1.09 Å); the most important structural parameters are given in Table 1. Since X-ray crystal data are not available for the complexes pcFe(14en)$_2$ (**1**) and pcFe(BuNH$_2$)$_2$ (**3**), the pc core was reproduced from the experimental geometry of pcFe(mepip)$_2$ (**2**), while in each case the axial ligands were placed at an Fe−N distance of 2.08 Å and their geometries were optimized at the semiempirical PM3 level[40] using the Polack−Ribiere algorithm[41] with help of the HyperChem 5.1Pro software.[42] Since the experimental geometries for pcFe(mepip)$_2$ (**2**) and pcFe(mepy)$_2$ (**5**) are quite similar, in spite of the pronounced difference between the axial ligands (mepip is a pure and strong σ-donor, while mepy is a moderate σ-donor and π-acceptor),[5b,12] the structural parameters of the pc core were considered to be representative of those of pcFe(14en)$_2$ (**1**) and pcFe(BuNH$_2$)$_2$ (**3**) as well. The choice of structural parameters for the axial ligands in pcFe(14en)$_2$ (**1**) and pcFe(BuNH$_2$)$_2$ (**3**) was not so straightforward. However, our electronic structural calculations on pcFe(14en)$_2$ (**1**) and pcFe(BuNH$_2$)$_2$ (**3**) showed the geometry of the axial ligands as obtained by optimization at the semiempirical PM3 level to be adequate for the prediction of Mössbauer and ^{1}H NMR spectral parameters. The molecular z axis was defined by the iron atom and the two atoms of the axial ligands directly coordinated to it. The rotation barriers of the axial ligands were calculated using the HyperChem 5.1Pro software at the molecular mechanics (MM+ force field) and semiempirical (PM3) levels. In all such model calculations, the phthalocyanine core and one axial ligand were kept fixed, while the other axial ligand was rotated in steps of 10° about the molecular z axis. The height of rotation barrier was then derived from the variation of the total energy as a function of the rotation angle. The NMR shielding tensor elements were calculated using the gauge-including atomic orbital (GIAO) method[43] with the help of the Gaussian-98W program. The aforementioned basis set with the hybrid B3LYP EC functional (Step 4) was used for the calculations of the NMR isotropic shifts.

Supporting Information Available: Spectroscopic and analytical data for the pcs used in this study. Atomic coordinates, equivalent isotropic displacement parameters, bond lengths and angles for **2**. Calculated orbital energies for complexes **1**−**8** using the LSDA and LDA EC functionals. Calculated, using the B3LYP hybrid EC functional and different basis sets for iron, Mössbauer quadrupole splittings in complexes **2** and **8** (see the note on the first page of this article).

Acknowledgments

The authors are grateful to Dr. E. V. Polshin for assistance in performing the Mössbauer experiments. V. N. N. thanks the JSPS

(grant no. P98418) and INTAS (grant no. 97-0791) for financial support. This research was partly supported by a Grant-in-Aid for Scientific Research (B) No. 11440192 and by funds for the Priority Area "Creation of Novel Delocalized Electron Systems", Award No. 12020206, from the Ministry of Education, Science, Sports, and Culture, Japan, and the Scandinavia−Japan Sasakawa Foundation to N. K.

[1] J. T. Groves, K. Shalyaev, J. Lee, in: *The Porphyrin Handbook*, vol. 4 (Eds.: K. M. Kadish, K. M. Smith, R. Guilard), Academic Press, San Diego, **2000**, pp. 17−40.

[2] O. L. Kaliya, E. A. Luk'yanets, in: *Fundamental Research in Homogeneous Catalysis*, vol. 1 (Ed.: E. A. Shilov), Gordon and Breach Sci. Publ., New York, London, **1986**, pp. 1−35.

[3] S. Neya, in: *Phthalocyanines: Properties and Applications*, vol. 4 (Eds.: C. C. Leznoff, A. B. P. Lever), VCH, New York, **1996**, pp. 447−479.

[4] [4a] V. N. Nemykin, V. Y. Chernii, V. V. Trachevskii, S. V. Volkov, *Ukr. Khim. Zh.* **1997**, *63*, 4. − [4b] N. A. Kostromina, V. Y. Chernii, V. N. Nemykin, I. V. Komarov, *Zh. Neorg. Khim.* **1995**, *40*, 1491. − [4c] B. W. Dale, R. J. R. Williams, P. R. Edwards, C. E. Johnson, *Trans. Faraday Soc.* **1968**, *64*, 3011. − [4d] C. K. Choy, J. R. Mooney, M. E. Kenney, *J. Magn. Reson.* **1979**, *35*, 1. − [4e] J. Maskasky, M. E. Kenney, *J. Am. Chem. Soc.* **1973**, *95*, 1443. − [4f] E. A. Ough, M. J. Stillman, *Inorg. Chem.* **1994**, *33*, 573. − [4g] J. J. Watkins, A. L. Balch, *Inorg. Chem.* **1975**, *14*, 2720. − [4h] D. A. Sweigart, *J. Chem. Soc., Dalton Trans.* **1976**, 1476. − [4i] M. Hanack, A. Hirsch, *Synth. Met.* **1989**, *29*, F9.

[5] [5a] V. N. Nemykin, V. Y. Chernii, E. V. Polshin, S. V. Volkov, *Ukr. Khim. Zh.* **1997**, *63*, 75. − [5b] V. N. Nemykin, A. E. Polshina, V. Y. Chernii, E. V. Polshin, N. Kobayashi, *J. Chem. Soc., Dalton Trans.* **2000**, 1019. − [5c] G. V. Ouedraogo, C. More, Y. Richard, D. Benlian, *Inorg. Chem.* **1981**, *20*, 4387. − [5d] M. Hanack, in: *Phthalocyanines: Properties and Applications*, vol. 2 (Eds.: C. C. Leznoff, A. B. P. Lever), VCH, New York, **1993**, pp. 43−96. − [5e] F. Calderazzo, S. Frediani, B. R. James, G. Pampaloni, K. J. Reimer, J. R. Sams, A. M. Serra, D. Vitalli, *Inorg. Chem.* **1982**, *21*, 2302. − [5f] B. W. Dale, R. J. R. Williams, P. R. Edwards, C. E. Johnson, *Trans. Faraday Soc.* **1968**, *64*, 620. − [5g] D. C. Grenoble, H. G. Drickamer, *J. Chem. Phys.* **1971**, *55*, 1624. − [5h] R. Taube, *Pure Appl. Chem.* **1974**, *38*, 427. − [5i] B. R. James, J. R. Sams, T. B. Tsin, K. J. Reimer, *J. Chem. Soc., Chem. Commun.* **1978**, 746.

[6] [6a] V. Valenti, P. Fantucci, F. Cariati, G. Micera, M. Petrera, N. Burriesci, *Inorg. Chim. Acta* **1988**, *148*, 191. − [6b] R. Taube, *Z. Chem.* **1966**, *6*, 8. − [6c] P. Coppens, L. Li, *J. Chem. Phys.* **1984**, *81*, 1983.

[7] [7a] F. Cariati, F. Marazzoni, M. Zocchi, *J. Chem. Soc., Dalton Trans.* **1978**, 1018. − [7b] C. Ercolani, F. Monacelli, S. Dzugan, V. L. Goedken, G. Pennesi, G. Rossi, *J. Chem. Soc., Dalton Trans.* **1991**, 1309. − [7c] W. Kalz, H. Homborg, H. Kuppers, B. J. Kennedy, K. S. Murray, *Z. Naturforsch.* **1984**, *39b*, 1478. − [7d] M. Hanack, G. Renz, J. Strahle, S. Schmid, *Chem. Ber.* **1988**, *121*, 1479. − [7e] M. Hanack, G. Renz, J. Strahle, S. Schmid, *J. Org. Chem.* **1991**, *56*, 3501. − [7f] F. Calderazzo, G. Pampaloni, D. Vitali, I. Collamati, J. Dessy, V. Fares, *J. Chem. Soc., Dalton Trans.* **1980**, 1965. − [7g] F. Calderazzo, G. Pampaloni, D. Vitali, G. Pelizzi, I. Collamati, S. Frediani, A. M. Serra, *J. Organomet. Chem.* **1980**, *191*, 217.

[8] R. G. Parr, W. Yang, *Density Functional Theory of Atoms and Molecules*, Oxford University Press, New York, **1989**.

[9] [9a] M. Grodzicki, H. Flint, H. Winkler, A. F. Walker, A. X. Trautwein, *J. Phys. Chem.* **1997**, *101*, 4202. − [9b] R. H. Havlin, N. Godbout, R. Salzmann, M. Wojdelski, W. Arnold, C. E. Schulz, E. Oldfield, *J. Am. Chem. Soc.* **1998**, *120*, 3144. − [9c] N. Godbout, R. H. Havlin, R. Salzmann, P. G. Debrunner, E. Oldfield, *J. Phys. Chem.* **1998**, *102*, 2342. − [9d] N. Godbout, L. K. Sanders, R. Salzmann, R. H. Havlin, M. Wojdelski, E. Oldfield, *J. Am. Chem. Soc.* **1999**, *121*, 3829.

[10] M. K. Safo, F. A. Walker, A. M. Raitsimring, W. P. Walters, D. P. Dolata, P. G. Debrunner, W. R. Scheidt, *J. Am. Chem. Soc.* **1994**, *116*, 7760; O. Q. Munro, P. S. Madlala, R. A. F. Warby, T. B. Seda, G. Hearne, *Inorg. Chem.* **1999**, *38*, 4724.

[11] J. P. Collman, J. L. Hoard, N. Kim, G. Lang, C. A. Reed, *J. Am. Chem. Soc.* **1975**, *97*, 2676.

[12] S. S. Fielder, M. C. Osborne, A. B. P. Lever, W. J. Pietro, *J. Am. Chem. Soc.* **1995**, *117*, 6990; V. N. Nemykin, A. E. Polshina, E. V. Polshin, N. Kobayashi, *Mendeleev Commun.* **2000**, 54.

[13] P. Gutlich, R. Link, A. X. Trautwein, *Mössbauer Spectroscopy and Transition Metal Chemistry*, Springer, Berlin, Heidelberg, **1978**; T. E. Cranshaw, B. W. Dale, G. O. Longworth, C. E. Johnson, *Mössbauer Spectroscopy and its Applications*, Cambridge University Press, Cambridge, **1985**.

[14] H. Paulsen, M. Krockel, M. Grodzicki, E. Bill, A. X. Trautwein, G. J. Liegh, J. Silver, *Inorg. Chem.* **1995**, *34*, 6244.

[15] M. Grodzicki, V. Männing, A. X. Trautwein, M. Friedt, *J. Phys. B* **1987**, *20*, 5595; M. Grodzicki, S. Lauer, A. X. Trautwein, A. Vera, *Adv. Chem. Ser.* **1981**, *194*, 3.

[16] C. H. Townes, B. P. Dailey, *J. Chem. Phys.* **1949**, *17*, 782.

[17] J. E. Ridley, M. C. Zerner, *Theor. Chim. Acta* **1976**, *42*, 223; A. D. Bacon, M. C. Zerner, *Theor. Chim. Acta* **1979**, *53*, 21.

[18] M. J. Stillman, T. Nyokong, in: *Phthalocyanines: Properties and Applications*, vol. 1 (Eds.: C. C. Leznoff, A. B. P. Lever), VCH, New York, **1989**, pp. 133−289.

[19] G. V. Ouedraogo, D. Benlian, L. Porte, *J. Chem. Phys.* **1980**, *73*, 642.

[20] A. B. P. Lever, *Inorganic Electronic Spectroscopy*, Elsevier, Amsterdam, **1984**.

[21] J. Cioslowski, A. Nanayakkara, M. Challacombe, *Chem. Phys. Lett.* **1993**, *203*, 137.

[22] *Density Functional Methods in Chemistry and Material Science* (Ed.: M. Springborg), Wiley, New York, **1997**.

[23] [23a] S. Yamamoto, J. Teraoka, H. Kashiwagi, *J. Chem. Phys.* **1988**, *88*, 303. − [23b] S. Obara, H. Kashiwagi, *J. Chem. Phys.* **1982**, *77*, 3155.

[24] [24a] P. S. Bagus, U. I. Walgren, J. Almlöf, *J. Chem. Phys.* **1976**, *64*, 2324. − [24b] A. X. Trautwein, F. E. Harris, A. J. Freeman, J. P. Desclaux, *Phys. Rev. B* **1975**, *11*, 4101. − [24c] L. R. B. Elton, A. Swift, *Proc. Phys. Soc. London* **1964**, *64*, 125.

[25] A. X. Trautwein, F. E. Harris, *Theor. Chim. Acta* **1973**, *30*, 45.

[26] J. R. Polam, J. L. Wright, K. A. Christensen, F. A. Walker, H. Flint, H. Winkler, M. Grodzicki, A. X. Trautwein, *J. Am. Chem. Soc.* **1996**, *118*, 5272.

[27] H. P. Luthi, J. H. Ammeter, J. Almlöf, K. Faergi, *J. Chem. Phys.* **1982**, *77*, 2002; J. B. Collins, A. Streitwieser, *J. Comput. Chem.* **1980**, *1*, 81.

[28] A. E. Reed, R. B. Weinstock, F. Weinhold, *J. Chem. Phys.* **1985**, *83*, 735; F. Weinhold, *Natural Bond Orbital Analysis Programs*, Board of Regents of the University of Wisconsin System, **1999**.

[29] R. Reschke, A. X. Trautwein, *Theor. Chim. Acta* **1978**, *47*, 85.

[30] G. M. Sheldrick, *SHELXTL-93*, *A Program for the Refinement of Crystal Structures*, University of Göttingen, Germany, **1993**.

[31] M. J. Frisch, G. W. Trucks, H. B. Schlegel, G. E. Scuseria, M. A. Robb, J. R. Cheeseman, V. G. Zakrzewski, J. A. Montgomery, R. E. Stratmann, J. C. Burant, S. Dapprich, J. M. Millam, A. D. Daniels, K. N. Kudin, M. C. Strain, O. Farkas, J. Tomasi, V. Barone, M. Cossi, R. Cammi, B. Mennucci, C. Pomelli, C. Adamo, S. Clifford, J. Ochterski, G. A. Petersson, P. Y. Ayala, Q. Cui, K. Morokuma, D. K. Malick, A. D. Rabuck, K. Raghavachari, J. B. Foresman, J. Cioslowski, J. V. Ortiz, B. B. Stefanov, G. Liu, A. Liashenko, P. Piskorz, I. Komaromi, R. Gomperts, R. L. Martin, D. J. Fox, T. Keith, M. A. Al-Laham, C. Y. Peng, A. Nanayakkara, C. Gonzalez, M. Challacombe, P. M. W. Gill, B. G. Johnson, W. Chen, M. W. Wong, J. L. Andres, M. Head-Gordon, E. S. Replogle, J. A. Pople, *Gaussian-98W (Revision A.7)*, Gaussian, Inc., Pittsburgh, PA, **1998**.

[32] P. J. Hay, *J. Chem. Phys.* **1977**, *66*, 4377; K. Raghavachari, G. W. Trucks, *J. Chem. Phys.* **1989**, *91*, 1062.

[33] A. D. Becke, *J. Chem. Phys.* **1993**, *98*, 5648.

[34] W. Kohn, L. J. Sham, *Phys. Rev. A* **1965**, *140*, 1133.

[35] S. H. Vosko, L. Wilk, M. Nusair, *Can. J. Phys.* **1980**, *98*, 1200.

[36] A. J. H. Wachters, *J. Chem. Phys.* **1970**, *52*, 1033.

[37] Basis sets were obtained from the *Extensible Computational Chemistry Environment Basis Set Database, Version 1.0*, as developed and distributed by the Molecular Science Computing Facility, Environment and Molecular Sciences Laboratory, which is a part of the Pacific Northwest Laboratory, P. O. Box 999, Richland, WA 99352, and is funded by the U.S. Depart-

ment of Energy under contract DE-AC06−76RLO 1830. Contact David Feller, Karen Schuchardt, or Don Jones for further information.
[38] M. W. Schmidt, K. K. Baldridge, J. A. Boatz, S. T. Elbert, M. S. Gordon, J. H. Jensen, S. Koseki, N. Matsunaga, K. A. Nguyen, S. J. Su, T. L. Windus, M. Dupuis, J. A. Montgomery, *J. Comput. Chem.* **1993**, *14*, 1347.
[39] P. Dufek, P. Bhala, K. Schwarz, *Phys. Rev. Lett.* **1995**, *75*, 3545.
[40] J. J. P. Stewart, *J. Comp. Aided Mol. Design* **1990**, *4*, 1.
[41] *HyperChem Computational Chemistry*, Hypercube, Inc., Gainesville, FL, **1996**.
[42] *HyperChem 5.1 Pro*, Hypercube, Inc., Gainesville, FL, USA, **1997**.
[43] K. Wolinski, J. F. Hilton, P. Pulay, *J. Am. Chem. Soc.* **1990**, *112*, 8251.

Received August 17, 2000
[I00321]